Elucidation of the *Aspergillus fumigatus* tRNA-derived RNA repertoire from conidia and mycelium.

Abdulrahman A. Kelani[1#], Xiaoqing Pan[1#], Matthew G. Blango[1*]

[1] Junior Research Group RNA Biology of Fungal Infections, Leibniz Institute for Natural Product Research and Infection Biology—Hans Knöll Institute (Leibniz-HKI), Jena, Germany.

[#] These authors contributed equally to this manuscript and are listed alphabetically.

Running Title: *A. fumigatus* produces abundant tRNA-derived RNAs.

Key Words: filamentous fungi, fungal pathogen, tRNA-derived RNAs, small RNA

*Correspondence: E-mail matthew.blango@leibniz-hki.de; Tel. +49 (0)3641-532 1072.

ABSTRACT

Aspergillus fumigatus is a ubiquitous filamentous fungus that causes devastating infections in severely immunocompromised individuals in the clinic. Pathogenesis relies in part on a combination of fine-tuned stress response pathways and rapid growth rate. Previous literature suggests that *A. fumigatus* produces a finite pool of small RNAs, consisting in part of tRNA-derived RNAs (tDRs). Here, we improve our understanding of the tDRs of *A. fumigatus* produced in conidia and mycelium using small RNA-sequencing and a cutting-edge tDR-sequencing approach. We find tDRs to be differentially abundant across fungal morphotypes, with specific fragments proving dominant in particular morphotypes (e.g., Asp(GTC)-5'tRH in conidia; His(GTG)-5'tRH in mycelium). Consistent with the literature, we observed distinct patterns of tDRs from nuclear- and mitochondria-derived tDRs and found tDR-seq to provide a modestly improved view of the tDRs of *A. fumigatus* over standard sRNA-seq. Ultimately, we have provided an improved description of the sRNA landscape of *A. fumigatus* and uncovered numerous small RNA species likely linked to gene regulation in this important human pathogen.

INTRODUCTION

Mature tRNAs and pre-tRNAs can be processed by cellular endonucleases to generate tRNA-derived RNAs (tDRs) of 10 to 50 nucleotides (nt) in length [1] (**Fig. S1**). This heterogeneous group of small RNAs (sRNAs) includes the 5' and 3' tRNA halves (tRHs), tRNA fragments (tRF) processed from the 5' (tRF-5) and 3' ends (tRF-3), and internal tRFs (i-tRF). The generation of tRHs (~31 to 40 nt) is multifactorial, but cellular stress is a well-described trigger of tRNA cleavage particularly in the anticodon loop, resulting in tRNA-derived, stress-induced fragments (tiRNAs) [2-5]. Enzymes like the RNase A ribonuclease angiogenin, and other endonucleases like RNase T2 or Rny1 in yeast cleave RNA, resulting ultimately in a 3'-phosphate (P)[6, 7]. Cleavage of mature tRNAs by angiogenin generates 5'-tRHs with a 5'-P and a 3'-terminal cyclic phosphate (cP), and 3'-tRHs with a 5'-hydroxyl (OH) and a 3'-terminal amino acid [8], in contrast to the RNase III enzyme Dicer that generate a 5'-P and a 3'-OH as in its canonical role in RNA interference (RNAi) [9]. tRF-5 and tRF-3 are 17 to 25 nt long products of mature tRNA cleavage at the 5' end D loop and 3' end T loop, and are produced by angiogenin or even Dicer in some species [10-13]. tRF-3 can be generated with or without the terminal CCA trinucleotide (tRF-3 CCA).

The biogenesis of tRFs and tRHs is dynamic across development [4, 14] and stress challenge [5, 15-17]. Previous work on the pathogenic fungus *Aspergillus fumigatus* small non-coding RNAs (ncRNA) revealed accumulation of tRHs over germination from conidia to hyphae [4]. Mature tRNA levels seemed unaffected; however, during the early stages of conidiogenesis, there is a rapid increase in

tRHs and a decrease in mature tRNA levels [4]. The full repertoire of tDRs remains untested, with potential functions unknown. tDRs can indeed perform a wide range of functions. For example, tRF-3 fragments can guide silencing of target mRNA via RNAi [18, 19] and the RNAi pathway is known to sometimes use sRNAs and tDRs as guides to induce both transcriptional gene silencing (TGS) of target gene loci or post transcriptional gene silencing (PTGS) of target RNA transcripts.

Here, we provide an improved characterization of the sRNA landscape of the filamentous fungus and World Health Organization critical priority pathogen, *A. fumigatus* [20]. Using sRNA-seq and tDR-seq, we reveal differential abundance of tDRs from *A. fumigatus* conidia (asexual spores) and mycelium (hyphal network).

RESULTS

The composition of *A. fumigatus* small RNAs is morphotype specific.

The sRNA biogenesis pathways of *A. fumigatus* remain poorly understood [21]. Using previously described knockout strains in the canonical RNA interference machinery (Δ*dclA*/*B*, Δ*ppdA*/*B*, and Δ*rrpA*/*B*) created in the wild-type CEA17Δ*akuB*^{KU80} background, we simultaneously profiled expression of both small ncRNA (this study) and mRNA [22] from the same biological samples across three conditions (conidia, 24 h mycelium, and 48 h mycelium; (**Fig. 1A**; **Dataset S1**)). We mapped the expression of distinct small ncRNA classes, including snRNA, snoRNA, tDRs, and other small ncRNAs (**Fig. 1B**). Across all the sequencing samples, rRNA made up the majority of the mapped reads, followed by short reads mapping to tRNA genes. In conidia, many reads mapped to rRNA, whereas the proportion of tDRs and other small ncRNAs increased in the mycelial samples, consistent with an expected, more diverse transcriptome in metabolically active mycelium.

Previous work in *A. fumigatus* revealed an abundance of tRHs produced during starvation [4]. In agreement we observed an increase in the relative abundance of nuclear-encoded 5'-tRHs from conidia to older mycelium; however, we also detected a large abundance of tRFs, likely generated by cleavage of either mature or precursor tRNA (e.g., by RNase T2). For nuclear-encoded tRFs, we noticed that the relative abundance of tRF-5 increases from conidia to 24-h-old and 48-h-old mycelium where nutrients are more limited, while the tRF-3 abundance decreases across those samples (**Fig. 1C**). However, within mitochondrial tDRs, reads mapped mostly to tRF-3, 5'-tRHs, and tRF-5 (**Fig. 1C**).

Next, we created normalized heat maps of abundance for the tDRs of each tRNA (**Fig. 2**; **Fig. S2**) as previously in the literature [23]. We observed clear differences in the relative abundance of tDRs from

each morphotype, suggesting differential stability or potentially poor ligation following cleavage. We observed differences in tDR biogenesis for some of the RNAi knockout strains, especially Δ*ppdA*/*B*, as compared to the wild type, but according to Benjamini-Hochberg-corrected p-values determined by *t* test, these were not significantly different. Nonetheless, in conidia, Δ*ppdA*/*B* appeared to produce fewer tRF-3, tRF-3 CCA, and tRF-5 derivatives from many of the tRNAs. Surprisingly, we observed minimal differences in the production of tDRs in Δ*dclA*/*B*, with most of the observed differences occurring for tRF-5 at 48 h. These results suggest that the RNAi machinery, particularly the Dicer-like proteins, play only a minor role in tRNA fragment production in *A. fumigatus* under standard growth conditions.

tDR-seq reveals altered patterns across fungal morphotypes.

The abundance of tDRs in our sRNA-seq together with the known difficulties of sequencing tRNAs using standard methodologies (e.g., poor adapter ligation and decreased reverse transcription efficiency) led us to perform a tRF & tiRNA-seq (here denoted tDR-seq) approach on wild-type fungal morphotypes, where RNA ends are repaired and common methylation modifications are removed to facilitate ligation and readthrough, respectively (**Fig. 3A**; **Dataset S2**). Although more reads mapped to rRNA fragments than in the sRNA-seq, a closer look at the distribution of tDRs indicated a higher proportion of tRHs compared to the sRNA-seq analysis for both the nuclear-encoded tRNAs and the mitochondria-encoded tRNAs (**Fig. 3B**). As compared to the tDR distribution from sRNA-seq (**Fig. 1C**), tDR-seq revealed more 3'tRHs relative to other tDRs (**Fig. 3B**). Interestingly, the relative abundance of the 5'tRHs with nuclear origin were much higher in the conidia (~75%) after the tDR-seq approach (**Fig. 3B**). Further analysis revealed that a majority (~95%) of tDRs identified in the conidia came from a particular Asp(GTC) nuclear-encoded tRNA, with the 5'tRH being the most abundant fragment (**Fig. 4A**). The length of the tRNA fragments was more consistent with tRHs for the nuclear-encoded tRNAs, but the mitochondria-encoded tDRs had a wider range, with a particular relative enrichment of smaller fragments in hyphae (**Fig. 3C**), consistent with the literature [23].

A heat map presenting the tDRs for each tRNA again revealed substantial differences in abundance and fragment distribution between tRNAs with different or even the same isoacceptor (**Fig. 4A**). Even though many of the detected tRHs derive from Asp(GTC), other tRNAs like His(GTG) and Pro(CGG) also produce a relatively high abundance of tRHs. Many of the nuclear-encoded tRNAs appeared to have stable tRF-3 CCA fragments, with the previously identified Tyr(GTA)-tRF-3 CCA being among the most abundant fragments (**Fig. 4A**; [22]). Curiously, tRF-3 CCA were almost completely lacking from

mitochondria-encoded tRNAs (**Fig. 4A and Fig. S2**), with a closer investigation only revealing a few poorly mapped reads. Further work will be required to experimentally validate this result.

DISCUSSION

Small ncRNAs are key regulators of gene expression and stress response in many organisms, including fungi. Here, we provide an improved description of the sRNA landscape of an important human fungal pathogen by leveraging sRNA-seq and tDR-seq. The pool of *A. fumigatus* tDRs appears to be heterogeneous, dynamic, and only partially dependent on the canonical RNAi machinery under standard growth conditions.

We initially performed sRNA-seq to evaluate the dynamics of small ncRNAs during two distinct morphological phases of *A. fumigatus* growth and identified expected classes of small ncRNAs, with rRNA and tDRs exhibiting the highest abundance in conidia and mycelium. Some previous studies have indicated that RNAi components like Dicer play a role in tDR biogenesis [10-12], but our results suggest that *A. fumigatus* Dicer-like proteins play only a minor role in biogenesis. Although, in comparison to the wild type, we observed a decrease in the production of some tDRs in the conidia of the Argonaute double knockout and an increase at later growth stages (i.e., 48-h-old hyphae). Argonautes are known to stabilize tRFs in some systems [13], and it remains possible that the total pool of mature tRNAs susceptible to cleavage is lower in the Argonaute double knockout strain, based on the downregulation of genes associated with transcription that we observed in previous work [22].

To better assess the tDR repertoire of *A. fumigatus*, we performed tDR-seq [24], which revealed an enriched pool of tRHs not detected with sRNA-seq, consistent with the literature [4]. The tDR-seq dataset revealed an abundance of rRNA reads, a smaller fraction of tDRs and other RNAs consistent with previous work [25], and a surprising absence of detection of tRF-3 CCA fragments derived from mitochondria-encoded tRNAs. An improved annotation of the *A. fumigatus* mitochondrial genome and further molecular work will be required to better assess these CCA-containing fragments. In conclusion, our study provides an improved view of tDR abundance and dynamics in *A. fumigatus* conidia and mycelium, which will likely be valuable in further defining the molecular biology of this important human pathogen.

MATERIALS AND METHODS

Strains, culture conditions, and RNA isolation

Throughout this study, *A. fumigatus* strains (**Table S1**) were cultivated on *Aspergillus* minimal medium (AMM) agar plates and liquid culture as described previously [22]. RNA isolation was performed exactly as described in [22] using TRIzol reagent.

Library preparation and sequencing

sRNA-seq libraries were prepared by Novogene using the TruSeq Small RNA Library Preparation Kit according to the manufacturer's protocol, then sequenced using NovaSeq 6000 instrument in a single-read, 50-bp based mode at 10 million reads of sequencing depth. For tDR-seq performed by CD Genomics (tRF&tiRNA-seq), the following treatments for modifications were performed: 1) 3'-aminoacyl (charged) deacylation to 3'-OH for 3' adaptor ligation, 2) 3'-cP removal to 3'-OH for 3' adaptor ligation, 3) 5'-OH (hydroxyl group) phosphorylation to 5'-P for 5'-adaptor ligation, and 4) m^1A and m^3C demethylation for efficient reverse transcription. Finally, RNA libraries were sequenced using an Illumina HiSeq 2500 instrument in a 50-bp single-read mode at 10 million reads of sequencing depth.

Data Analysis

TrimGalore version 0.6.8 was used for quality checks and removing adaptors of sequencing reads. Sequencing results were analyzed with unitas v. 1.7.0 [26] using default parameters and *Aspergillus fumigatus* A1163 ASM15014v1 as reference genome. *A. fumigatus* nuclear tRNAs were referenced from GtRNAdb [27], mitochondrial tRNAs were scanned from the mitochondrial genome [28] using the 27 tRNAs predicted by tRNAscan-SE [29]. All analyses were performed using "R" version 4.3.1 (2023-06-16) and Rstudio (2022-02-02), an integrated development environment (IDE) for R. Figures were drawn with the ggplot2 package (version 3.4.2) in R. *P*-values were determined by ANOVA or two-tailed Student's t-tests where appropriate and differences between the groups were considered significant at a *P*-value of <0.05.

Data availability

The sRNA-seq data are available under NCBI Gene Expression Omnibus (GEO) identifier GSE267454. These data were collected simultaneously with previously published mRNA-seq data [22] available using identifier GSE223618. The tDR-seq data is available under identifier GSE267453.

ACKNOWLEDGEMENTS

We would like to thank Pamela Lehenberger and Bhawana Israni for excellent technical assistance and Axel Brakhage, Alexander Bruch, and Xiuqiang Chen for helpful discussions. The work presented here was generously supported by the Federal Ministry for Education and Research (BMBF: https://www.bmbf.de/), Germany, Project FKZ 01K12012 “RFIN – RNA-Biologie von Pilzinfektionen”. The funders had no role in the design of the study. The authors declare no conflicts of interest.

FIGURES AND FIGURE LEGENDS

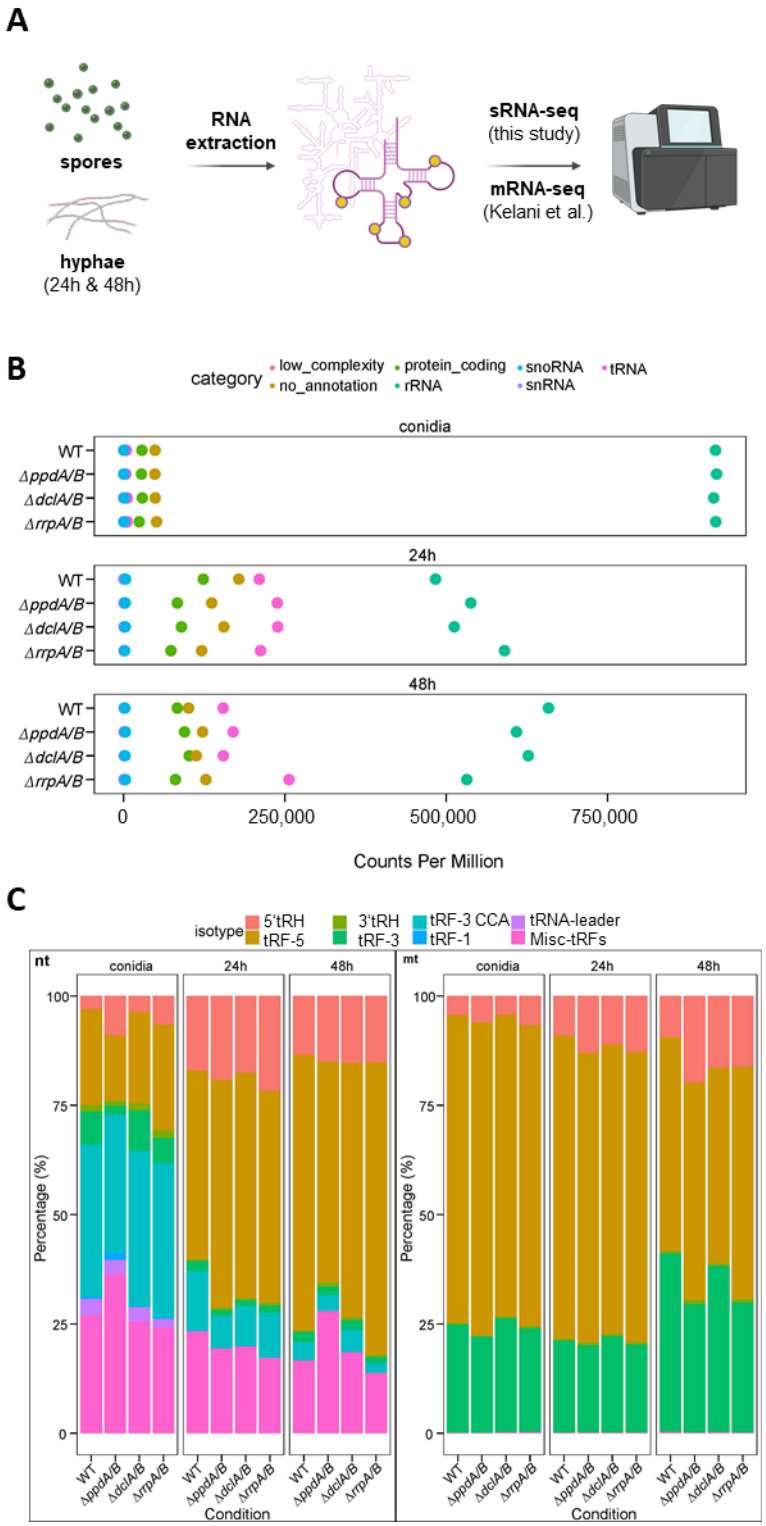

FIG 1. Small RNA abundance in *A. fumigatus* conidia and mycelium.

(A) Strains and conditions profiled in this study. The wild-type (CEA17 Δ*akuB*^{ku80}) and three mutant strains (Δ*ppdA/B*, Δ*dclA/B*, Δ*rrpA/B*) were collected (n = 3 biological replicates per condition). RNA samples were collected from fungal conidia and hyphae (24 hours and 48 hours) and Illumina sequenced. **(B)** Coverage of small ncRNA types within the profiled samples. Small ncRNAs were

annotated with low complexity, no annotation, protein coding, rRNA, snoRNA, snRNA, and tRNA (including nuclear tRNA and mitochondrial tRNA). **(C)** Comparison of tDR relative abundance across samples, and between wild-type and RNAi mutants.

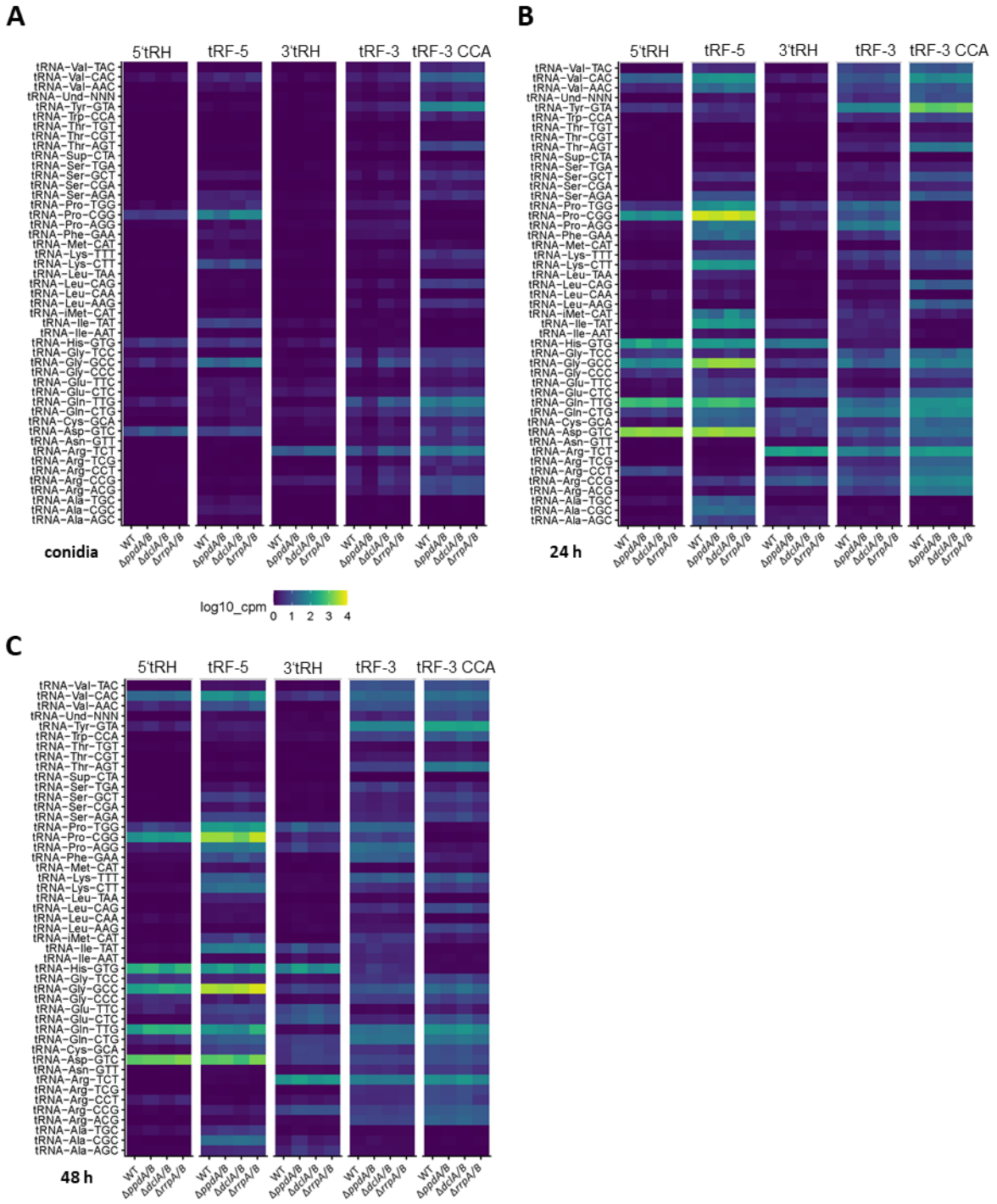

FIG 2. Expression of tDRs in *A. fumigatus* conidia and mycelium.

Heatmap showing abundance of nuclear tRNA (nt) tDR species and their tRNA origin (tRNA Transcript ID =1, Gene locus ID =1) across sampled morphotypes: **(A)** Conidia, **(B)** 24 hours-, and **(C)** 48 hours-old-mycelium of wild-type and RNAi double knockouts as determined by sRNA-seq. Plots show counts per million mapped reads based on fractionated counts produced with unitas v. 1.7.0 [26]. n = 3 biological replicates per condition.

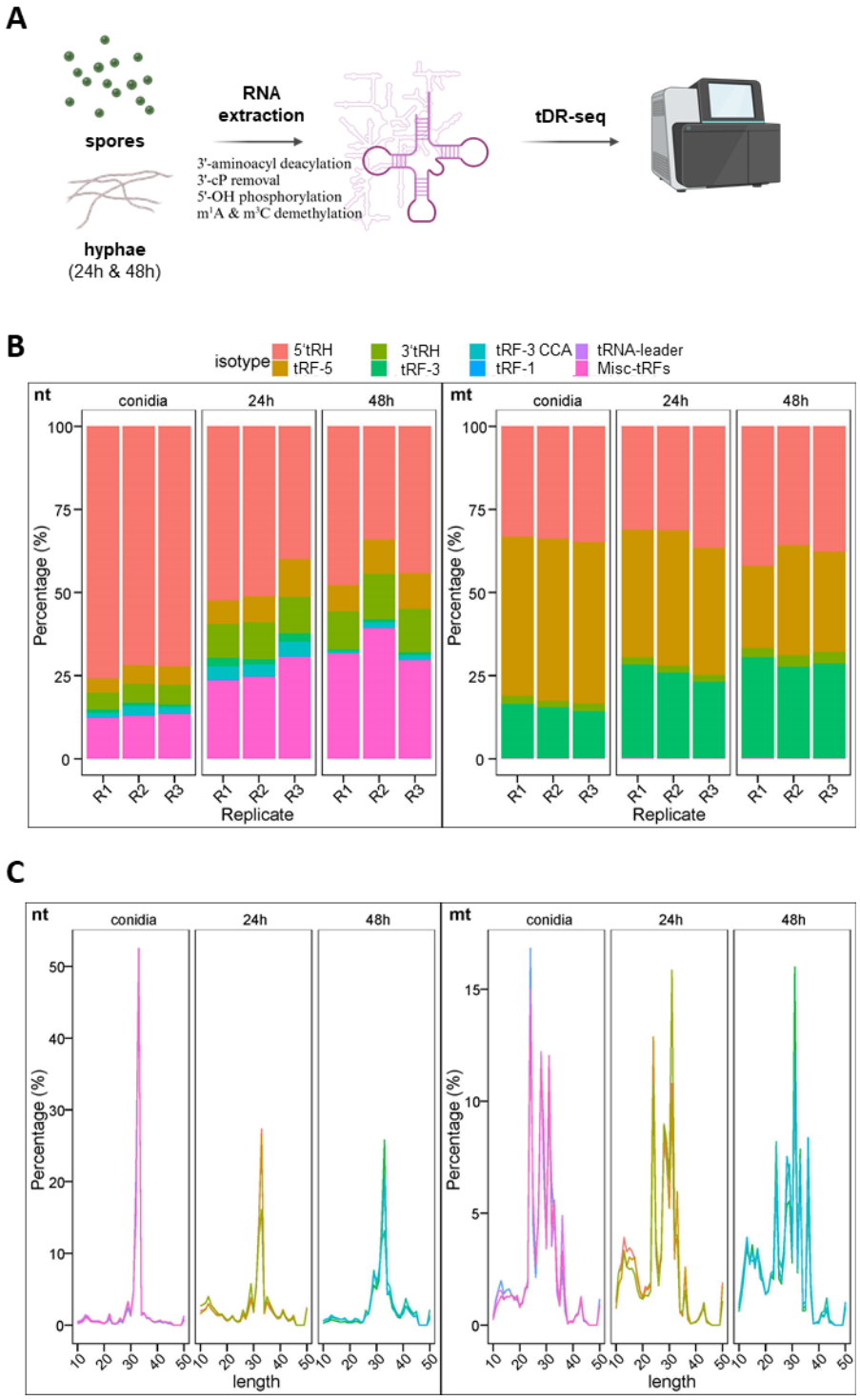

FIG 3. Dynamics of tDR expression in *A. fumigatus* conidia and mycelium revealed by tDR-seq. **(A)** RNA samples (n = 3) were collected from wild-type *A. fumigatus* conidia and hyphae. Samples were pre-treated to remove specific modifications and resolve tDR ends prior to library preparation. RNA molecules of up to 50 nt were selected for tDR-seq using Illumina sequencing. **(B)** Relative abundance of different tDRs across samples. **(C)** Average tDR length identified across samples for either ntRNA-derived (**left**) or mtRNA-derived (**right**) fragments.

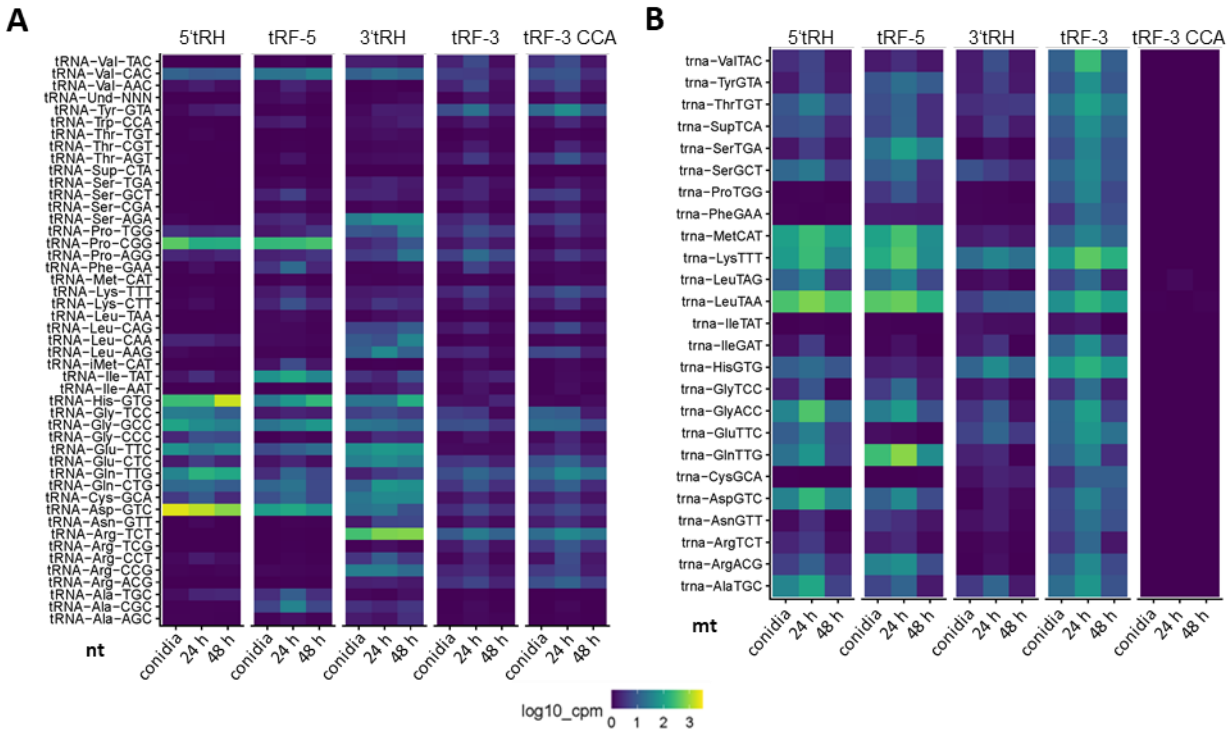

FIG 4. tDR-seq reveals changes in abundance of specific tDR fragments across morphotypes. Heatmap showing abundance of **(A)** nuclear- (nt) and **(B)** mitochondria-encoded (mt) tDR species and their tRNA of origin (tRNA Transcript ID =1, Gene locus ID =1) across sampled conidia and mycelium timepoints. Plots show counts per million mapped reads based on fractionated counts produced with unitas v. 1.7.0 [26]. n = 3 biological replicates per condition.

REFERENCES

1. Tyczewska A, Grzywacz K. tRNA-derived fragments as new players in regulatory processes in yeast. Yeast. 2022. Epub 2022/11/18. doi: 10.1002/yea.3829. PubMed PMID: 36385711.
2. Donovan J, Rath S, Kolet-Mandrikov D, Korennykh A. Rapid RNase L-driven arrest of protein synthesis in the dsRNA response without degradation of translation machinery. RNA. 2017;23(11):1660-71. Epub 2017/08/16. doi: 10.1261/rna.062000.117. PubMed PMID: 28808124; PubMed Central PMCID: PMCPMC5648034.
3. Ivanov P, Emara MM, Villen J, Gygi SP, Anderson P. Angiogenin-induced tRNA fragments inhibit translation initiation. Mol Cell. 2011;43(4):613-23. Epub 2011/08/23. doi: 10.1016/j.molcel.2011.06.022. PubMed PMID: 21855800; PubMed Central PMCID: PMCPMC3160621.
4. Jochl C, Rederstorff M, Hertel J, Stadler PF, Hofacker IL, Schrettl M, et al. Small ncRNA transcriptome analysis from *Aspergillus fumigatus* suggests a novel mechanism for regulation of protein synthesis. Nucleic Acids Res. 2008;36(8):2677-89. Epub 2008/03/19. doi: 10.1093/nar/gkn123. PubMed PMID: 18346967; PubMed Central PMCID: PMCPMC2377427.
5. Thompson DM, Lu C, Green PJ, Parker R. tRNA cleavage is a conserved response to oxidative stress in eukaryotes. RNA. 2008;14(10):2095-103. Epub 2008/08/23. doi: 10.1261/rna.1232808. PubMed PMID: 18719243; PubMed Central PMCID: PMCPMC2553748.

6. Luhtala N, Parker R. T2 Family ribonucleases: ancient enzymes with diverse roles. Trends Biochem Sci. 2010;35(5):253-9. Epub 2010/03/02. doi: 10.1016/j.tibs.2010.02.002. PubMed PMID: 20189811; PubMed Central PMCID: PMCPMC2888479.
7. Loveland AB, Koh CS, Ganesan R, Jacobson A, Korostelev AA. Structural mechanism of angiogenin activation by the ribosome. Nature. 2024. Epub 20240508. doi: 10.1038/s41586-024-07508-8. PubMed PMID: 38718836.
8. Honda S, Loher P, Shigematsu M, Palazzo JP, Suzuki R, Imoto I, et al. Sex hormone-dependent tRNA halves enhance cell proliferation in breast and prostate cancers. Proc Natl Acad Sci U S A. 2015;112(29):E3816-25. Epub 2015/07/01. doi: 10.1073/pnas.1510077112. PubMed PMID: 26124144; PubMed Central PMCID: PMCPMC4517238.
9. Carthew RW, Sontheimer EJ. Origins and Mechanisms of miRNAs and siRNAs. Cell. 2009;136(4):642-55. Epub 2009/02/26. doi: 10.1016/j.cell.2009.01.035. PubMed PMID: 19239886; PubMed Central PMCID: PMCPMC2675692.
10. Babiarz JE, Ruby JG, Wang Y, Bartel DP, Blelloch R. Mouse ES cells express endogenous shRNAs, siRNAs, and other Microprocessor-independent, Dicer-dependent small RNAs. Genes Dev. 2008;22(20):2773-85. Epub 2008/10/17. doi: 10.1101/gad.1705308. PubMed PMID: 18923076; PubMed Central PMCID: PMCPMC2569885.
11. Cole C, Sobala A, Lu C, Thatcher SR, Bowman A, Brown JW, et al. Filtering of deep sequencing data reveals the existence of abundant Dicer-dependent small RNAs derived from tRNAs. RNA. 2009;15(12):2147-60. Epub 2009/10/24. doi: 10.1261/rna.1738409. PubMed PMID: 19850906; PubMed Central PMCID: PMCPMC2779667.
12. Haussecker D, Huang Y, Lau A, Parameswaran P, Fire AZ, Kay MA. Human tRNA-derived small RNAs in the global regulation of RNA silencing. RNA. 2010;16(4):673-95. Epub 2010/02/26. doi: 10.1261/rna.2000810. PubMed PMID: 20181738; PubMed Central PMCID: PMCPMC2844617.
13. Kuscu C, Kumar P, Kiran M, Su Z, Malik A, Dutta A. tRNA fragments (tRFs) guide Ago to regulate gene expression post-transcriptionally in a Dicer-independent manner. RNA. 2018;24(8):1093-105. Epub 2018/05/31. doi: 10.1261/rna.066126.118. PubMed PMID: 29844106; PubMed Central PMCID: PMCPMC6049499.
14. Haiser HJ, Karginov FV, Hannon GJ, Elliot MA. Developmentally regulated cleavage of tRNAs in the bacterium *Streptomyces coelicolor*. Nucleic Acids Res. 2008;36(3):732-41. Epub 2007/12/18. doi: 10.1093/nar/gkm1096. PubMed PMID: 18084030; PubMed Central PMCID: PMCPMC2241913.
15. Hsieh LC, Lin SI, Kuo HF, Chiou TJ. Abundance of tRNA-derived small RNAs in phosphate-starved *Arabidopsis* roots. Plant Signal Behav. 2010;5(5):537-9. Epub 2010/04/21. doi: 10.4161/psb.11029. PubMed PMID: 20404547; PubMed Central PMCID: PMCPMC7080466.
16. Lee SR, Collins K. Starvation-induced cleavage of the tRNA anticodon loop in *Tetrahymena thermophila*. J Biol Chem. 2005;280(52):42744-9. Epub 2005/11/08. doi: 10.1074/jbc.M510356200. PubMed PMID: 16272149.
17. Yamasaki S, Ivanov P, Hu GF, Anderson P. Angiogenin cleaves tRNA and promotes stress-induced translational repression. J Cell Biol. 2009;185(1):35-42. Epub 2009/04/01. doi: 10.1083/jcb.200811106. PubMed PMID: 19332886; PubMed Central PMCID: PMCPMC2700517.
18. Maute RL, Schneider C, Sumazin P, Holmes A, Califano A, Basso K, Dalla-Favera R. tRNA-derived microRNA modulates proliferation and the DNA damage response and is down-regulated in B cell lymphoma. Proc Natl Acad Sci U S A. 2013;110(4):1404-9. Epub 2013/01/09. doi: 10.1073/pnas.1206761110. PubMed PMID: 23297232; PubMed Central PMCID: PMCPMC3557069.
19. Thompson DM, Parker R. The RNase Rny1p cleaves tRNAs and promotes cell death during oxidative stress in *Saccharomyces cerevisiae*. J Cell Biol. 2009;185(1):43-50. Epub 2009/04/01. doi: 10.1083/jcb.200811119. PubMed PMID: 19332891; PubMed Central PMCID: PMCPMC2700514.
20. Fisher MC, Denning DW. The WHO fungal priority pathogens list as a game-changer. Nature Reviews Microbiology. 2023;21(4):211-2. doi: 10.1038/s41579-023-00861-x.

21. Mouyna I, Henry C, Doering TL, Latge JP. Gene silencing with RNA interference in the human pathogenic fungus *Aspergillus fumigatus*. FEMS Microbiol Lett. 2004;237(2):317-24. Epub 2004/08/24. doi: 10.1016/j.femsle.2004.06.048. PubMed PMID: 15321679.
22. Kelani AA, Bruch A, Rivieccio F, Visser C, Kruger T, Weaver D, et al. Disruption of the *Aspergillus fumigatus* RNA interference machinery alters the conidial transcriptome. RNA. 2023;29(7):1033-50. Epub 2023/04/06. doi: 10.1261/rna.079350.122. PubMed PMID: 37019633; PubMed Central PMCID: PMCPMC10275271.
23. Isakova A, Fehlmann T, Keller A, Quake SR. A mouse tissue atlas of small noncoding RNA. Proc Natl Acad Sci U S A. 2020;117(41):25634-45. Epub 2020/09/27. doi: 10.1073/pnas.2002277117. PubMed PMID: 32978296; PubMed Central PMCID: PMCPMC7568261.
24. Zhang J, Li L, Luo L, Yang X, Zhang J, Xie Y, et al. Screening and potential role of tRFs and tiRNAs derived from tRNAs in the carcinogenesis and development of lung adenocarcinoma. Oncol Lett. 2021;22(1):506. Epub 2021/05/15. doi: 10.3892/ol.2021.12767. PubMed PMID: 33986867; PubMed Central PMCID: PMCPMC8114470.
25. Gustafsson HT, Galan C, Yu T, Upton HE, Ferguson L, Kaymak E, et al. Deep sequencing of yeast and mouse tRNAs and tRNA fragments using OTTR. bioRxiv. 2022:2022.02.04.479139. doi: 10.1101/2022.02.04.479139.
26. Gebert D, Hewel C, Rosenkranz D. unitas: the universal tool for annotation of small RNAs. BMC Genomics. 2017;18(1):644. doi: 10.1186/s12864-017-4031-9.
27. Thornlow BP, Armstrong J, Holmes AD, Howard JM, Corbett-Detig RB, Lowe TM. Predicting transfer RNA gene activity from sequence and genome context. Genome Res. 2020;30(1):85-94. Epub 2019/12/21. doi: 10.1101/gr.256164.119. PubMed PMID: 31857444; PubMed Central PMCID: PMCPMC6961574.
28. Joardar V, Abrams NF, Hostetler J, Paukstelis PJ, Pakala S, Pakala SB, et al. Sequencing of mitochondrial genomes of nine *Aspergillus* and *Penicillium* species identifies mobile introns and accessory genes as main sources of genome size variability. BMC Genomics. 2012;13(1):698. doi: 10.1186/1471-2164-13-698.
29. Chan PP, Lin BY, Mak AJ, Lowe TM. tRNAscan-SE 2.0: improved detection and functional classification of transfer RNA genes. Nucleic Acids Res. 2021;49(16):9077-96. Epub 2021/08/22. doi: 10.1093/nar/gkab688. PubMed PMID: 34417604; PubMed Central PMCID: PMCPMC8450103.